

RESEARCH ARTICLE

Increased glucocorticoid concentrations in early life cause mitochondrial inefficiency and short telomeres

Stefania Casagrande^{1,*}, Antoine Stier^{2,3}, Pat Monaghan², Jasmine L. Loveland⁴, Winifred Boner², Sara Lupi^{1,5}, Rachele Trevisi¹ and Michaela Hau^{1,6}


ABSTRACT

Telomeres are DNA structures that protect chromosome ends. However, telomeres shorten during cell replication and at critically low lengths can reduce cell replicative potential, induce cell senescence and decrease fitness. Stress exposure, which elevates glucocorticoid hormone concentrations, can exacerbate telomere attrition. This phenomenon has been attributed to increased oxidative stress generated by glucocorticoids ('oxidative stress hypothesis'). We recently suggested that glucocorticoids could increase telomere attrition during stressful periods by reducing the resources available for telomere maintenance through changes in the metabolic machinery ('metabolic telomere attrition hypothesis'). Here, we tested whether experimental increases in glucocorticoid levels affected telomere length and mitochondrial function in wild great tit (*Parus major*) nestlings during the energy-demanding early growth period. We monitored resulting corticosterone (Cort) concentrations in plasma and red blood cells, telomere lengths and mitochondrial metabolism (metabolic rate, proton leak, oxidative phosphorylation, maximal mitochondrial capacity and mitochondrial inefficiency). We assessed oxidative damage caused by reactive oxygen species (ROS) metabolites as well as the total non-enzymatic antioxidant protection in plasma. Compared with control nestlings, Cort-nestlings had higher baseline corticosterone, shorter telomeres and higher mitochondrial metabolic rate. Importantly, Cort-nestlings showed increased mitochondrial proton leak, leading to a decreased ATP production efficiency. Treatment groups did not differ in oxidative damage or antioxidants. Hence, glucocorticoid-induced telomere attrition is associated with changes in mitochondrial metabolism, but not with ROS production. These findings support the hypothesis that shortening of telomere length during stressful periods is mediated by glucocorticoids through metabolic rearrangements.

KEY WORDS: Mitochondria, Metabolism, Proton leak, Oxidative stress, Telomere, Nr3c1, Glucocorticoid receptor

¹Max Planck Institute for Ornithology, Evolutionary Physiology Group, 82319 Seewiesen, Germany. ²Institute of Biodiversity Animal Health and Comparative Medicine, University of Glasgow, Glasgow, G12 8QQ, UK. ³Department of Biology, University of Turku, FI-20014 Turku, Finland. ⁴Max Planck Institute for Ornithology, Behavioural Genetics and Evolutionary Ecology Group, 82319 Seewiesen, Germany. ⁵Konrad Lorenz Institute of Ethology, University of Veterinary Medicine, Vienna, A-1160 Vienna, Austria. ⁶Department of Biology, University of Konstanz, D-78464 Konstanz, Germany.

*Author for correspondence (scasagrande@orn.mpg.de)

 S.C., 0000-0002-4264-8062; A.S., 0000-0002-5445-5524; P.M., 0000-0003-2430-0326; S.L., 0000-0003-1789-9406; R.T., 0000-0002-8206-3093; M.H., 0000-0002-3836-4083

Received 28 January 2020; Accepted 4 June 2020

INTRODUCTION

Life-history traits can be shaped by environmental conditions experienced during early development (e.g. Monaghan, 2008; Monaghan and Haussmann, 2015). A biomarker that has been used to assess how early life conditions can influence later life health and longevity is telomere dynamics (Monaghan and Haussmann, 2006; Monaghan, 2010). In vertebrates, telomeres are non-coding DNA repeats of $(T_2AG_3)_n$ that form complexes with proteins and RNA at the chromosome ends. They signal the true chromosome ends to the DNA repair machinery, and also protect coding sequences from the loss caused by the intrinsically incomplete DNA replication at the end of the lagging strands during cell division. After reaching a critical length, the consequent telomere dysfunction can trigger a DNA damage response, induce apoptosis or cause a state of cell senescence through the arrest of cell replication (Passos et al., 2007; Blackburn et al., 2015). Therefore, telomeres play a fundamental role in maintaining genomic integrity and in affecting cellular functioning. In addition to the end-replication loss, the degree of shortening during cell division is also influenced by exposure to stressful events (Haussmann and Marchetto, 2010; Blackburn and Epel, 2012; Boonekamp et al., 2014; Monaghan, 2014; Hau et al., 2015; Haussmann and Heidinger, 2015; Nettle et al., 2015; Eastwood et al., 2018; Whittemore et al., 2019; Wood and Young, 2019). Short telomere lengths or high telomere attrition rates in early life and adulthood are associated with lower life expectancy and higher disease risk in various species including humans (Bize et al., 2009; Heidinger et al., 2012; López-Otín et al., 2013). A causal link between telomere length and organismal viability and biological ageing is suggested by studies that manipulated the length of telomeres in laboratory mice (de Jesus et al., 2011; Bernardes de Jesus et al., 2012; Varela et al., 2016; Muñoz-Lorente et al., 2019). In the most recent study, mice generated from embryonic stem cells with hyper-long telomeres showed improved glucose metabolism, a slower ageing rate and an increased life span, indicating a causal role for long telomeres in improving individual viability (Muñoz-Lorente et al., 2019). Thus, the pattern and pace of telomere dynamics can have significant consequences for phenotypes and for the fitness prospects of individuals.

In the majority of endothermic vertebrates, the highest telomere attrition rates are observed during early development (reviewed in Monaghan and Ozanne, 2018). This is in part a consequence of high cell division rates, the repeated exposure of DNA to potentially damaging conditions within the cell, and limited telomere restoration in most somatic tissues (Monaghan and Ozanne, 2018). In addition, telomere attrition is often exacerbated during stressful conditions, i.e. when concentrations of glucocorticoid hormones are up-regulated (Haussmann and Heidinger, 2015; Angelier et al., 2018; Monaghan and Ozanne, 2018; Casagrande and Hau, 2019). Glucocorticoids adjust physiological and behavioural responses to cope with predictable as well as

unpredictable variations in internal and external conditions (Hau et al., 2016; Romero and Wingfield, 2016). Exposure to stressful conditions like food limitation, extreme temperatures, predator presence, social competition, diseases or noxious stimuli can result in an up-regulation of circulating concentrations of glucocorticoid hormones (Sapolsky et al., 2000; Romero, 2004; Hau et al., 2016; Romero and Wingfield, 2016); this often is associated with increased telomere loss (Hau et al., 2015; Haussmann and Heidinger, 2015; Angelier et al., 2018; Casagrande and Hau, 2019). The effects of glucocorticoids on telomeres have been documented in several endothermic vertebrates in both experimental and correlational studies (Kotrschal et al., 2007; Schultner et al., 2014; Stier et al., 2014b; Zalli et al., 2014; Angelier et al., 2018; Casagrande and Hau, 2019), with the best studied wild vertebrate models being avian species (Haussmann et al., 2012; Herborn et al., 2014; Tissier et al., 2014; Quirici et al., 2016).

However, the route by which glucocorticoids influence telomere loss is unclear. Thus far, the focus has been on oxidative damage as the primary mechanism by which glucocorticoids induce telomere attrition ('oxidative stress hypothesis'; Haussmann and Marchetto, 2010; Monaghan, 2014; Haussmann and Heidinger, 2015; Angelier et al., 2018). Telomeres are particularly vulnerable to high concentrations of pro-oxidants (Von Zglinicki, 2002; Monaghan and Ozanne, 2018), which can result from accelerated metabolism; for example, following growth spurts or glucocorticoid increases (Geiger et al., 2012). Glucocorticoids are posited to increase the production of reactive oxygen species (ROS) by enhancing metabolic rate, and by regulating endogenous antioxidant defences especially by increasing or decreasing the activity of antioxidant enzymes (Costantini et al., 2011; Haussmann and Heidinger, 2015; Angelier et al., 2018). However, increased metabolic rates can actually downregulate ROS production (Salin et al., 2015) and several recent studies have not confirmed that glucocorticoids affect enzymatic or non-enzymatic antioxidants or oxidative damage (Lendvai et al., 2014; Casagrande and Hau, 2018; Vitousek et al., 2018). More generally, while telomere attrition appears to be increased by oxidative stress – although evidence is stronger for *in vitro* (Von Zglinicki, 2002; but see Romano et al., 2013; Monaghan and Ozanne, 2018) than *in vivo* studies (Boonekamp et al., 2017; but see Reichert and Stier, 2017) – the mechanistic pathway whereby this occurs is unclear.

We recently suggested that one major pathway by which glucocorticoids may impact telomere dynamics is through the efficiency of cellular energy metabolism ('metabolic telomere attrition hypothesis'; Casagrande and Hau, 2019). Glucocorticoids are known to adjust metabolic processes at various organismal levels (Hau et al., 2016; Jimeno et al., 2017; 2018), but their exact role in regulating cellular metabolism, such as mitochondrial functioning, is still largely unresolved. However, it is known that glucocorticoid receptors can influence mitochondrial gene expression (Psarra and Sekeris, 2009; Koch et al., 2017). Mitochondria play a central role in cellular energy metabolism by using oxygen and nutrients to maintain a membrane potential that is required for adenosine triphosphate (ATP) production, the chemical energy used to power costly processes like growth, self-maintenance, reproduction and stress responses. Mitochondrial metabolic processes also include proton leak, a thermogenic backflow of protons that does not lead to ATP production (Jastroch et al., 2010). This 'inefficiency' of the mitochondria in producing heat instead of chemical energy may serve to protect the cell from the oxidative actions of ROS that arise as a by-product of the aerobic metabolism ('uncouple to survive' hypothesis; Brand,

2000; see Discussion for further details). Any cellular responses activated during stressful conditions are expected to be accompanied by increased mitochondrial energy production via oxidative phosphorylation. It has also been suggested that, during stressful times, proton leak should increase to produce heat (e.g. to support fever responses) and thereby reduce ATP production, while a controlled generation of ROS following increases in metabolic rate could serve signalling functions (Manoli et al., 2007; Picard et al., 2018). When stressful conditions are severe or long lasting and mitochondrial energy reserves are depleted, mitochondria can become dysfunctional (Manoli et al., 2007). Dysfunctionality leads to decreased ATP production, uncontrolled ROS generation and the induction of an apoptotic cascade aimed to enhance cell adaptation (Manoli et al., 2007; Eisner et al., 2018). Mitochondria dysfunctionality is often associated with telomere attrition, as observed in murine skeletal myoblasts (Guha et al., 2018), while restoration of impaired mitochondria leads to telomere restoration in mouse cardiomyocytes at a post-mitotic stage (Chang et al., 2016). Telomere maintenance is presumed to be costly (Young, 2018; Casagrande and Hau, 2019), which may aggravate energy limitations – especially during growth, when new cells are being produced at high rates (Monaghan and Ozanne, 2018; Casagrande and Hau, 2019). Any mitochondrial inefficiency, potentially induced by glucocorticoids, might further intensify energetic bottlenecks during this critical phase of life. The metabolic telomere attrition hypothesis therefore proposes the existence of a link between glucocorticoids and mitochondria in modulating the rate of telomere loss (Casagrande and Hau, 2019), which has not yet been directly tested. There exists evidence for some connection between mitochondria and glucocorticoids, as in laboratory rats the synthetic glucocorticoid dexamethasone can increase proton leak by 40% (Roussel et al., 2003), and in king penguins (*Aptenodytes patagonica*), natural glucocorticoid concentrations correlate positively with mitochondrial proton leak (Stier et al., 2019c). However, the direction of the interactions among glucocorticoids, mitochondria and telomeres is still unclear.

The aim of the current study was to experimentally investigate the effect of glucocorticoids on cell metabolic rate and to test the basic premise of the metabolic telomere attrition hypothesis, that the exacerbation of telomere attrition during early life by elevated glucocorticoid concentrations can involve metabolic adjustments independently of oxidative stress (Casagrande and Hau, 2019). One prediction of the hypothesis is that a reduction in the efficiency of ATP production per molecule of oxygen induced by glucocorticoids during a protracted stress exposure results in a reduction in ATP-dependent resources, like enzymes, proteins and nucleotides, being available for telomere maintenance. Telomere maintenance is crucial for the functioning of cells independently of their replicative potential. The most important reason is probably the signalling role of telomeres in the DNA damage response. This response is mediated by a network of proteins that has also been found in white blood cells (Wang et al., 2020), blood mononuclear cells (Carroll et al., 2016) and avian red blood cells (RBCs) (Meitern et al., 2014). We conducted our experiment in a wild avian species during the rapid growth phase of early development, when telomeres are supposed to be most vulnerable to oxidative stress because of the high rate of cell replication in the proliferative tissues from which they originate (i.e. bone marrow) – probably the only phase in the cell cycle when pro-oxidants can induce a loss of telomeric nucleotides because the DNA is unfolded and exposed to the actions of ROS (Von Zglinicki et al., 2000; Reichert and Stier, 2017). Although RBCs cannot replicate, telomere dynamics are

important for the functioning of these metabolically active cells because of the signalling role of telomeres in regulating cell metabolism (Sahin and DePinho, 2012; Ye et al., 2014; Casagrande and Hau, 2019; Zheng et al., 2019). We provided great tit (*Parus major* Linnaeus 1758) nestlings, a fast-growing species, with a daily oral dose of corticosterone (the main glucocorticoid in birds) for 10 days until the end of their post-hatching development. This manipulation mimics natural repeated increases in corticosterone, as usually observed during recurring stressful periods (Spencer and Verhulst, 2007). We compared nestlings receiving corticosterone (Cort-nestlings) with siblings from the same nest receiving only the oil vehicle (vehicle-nestlings) and with nestlings raised in undisturbed nests (control-nestlings). We examined the effectiveness and specificity of the corticosterone treatment, as well as the impact of frequent handling by measuring plasma concentrations of corticosterone, and the expression of the glucocorticoid receptor gene in RBCs (which is expected to be upregulated when birds are exposed to stressors; Lattin and Romero, 2014). In birds, RBCs are nucleated, allowing us to measure mitochondrial metabolic rate, oxidative phosphorylation and proton leak in erythrocytes (Stier et al., 2017). Avian RBC mitochondrial traits have been shown to be repeatable and correlated with those measured in pectoral muscle (Stier et al., 2017). A study on pied flycatchers (*Ficedula hypoleuca*) also showed that RBC mitochondrial functions are plastic traits that can adjust to different life-history stages and the energetic needs associated with those (Stier et al., 2019a). We also measured ROS-derived hydroperoxides and total non-enzymatic antioxidant in the plasma as an indicator of ROS production by mitochondrial aerobic metabolism. Finally, we recorded growth rate, which is usually decreased by glucocorticoids (Spencer and Verhulst, 2008; Tissier et al., 2014; Glazier, 2015). However, increased growth rate could reduce telomere length via a faster cell division rate and a higher generation of ROS (Monaghan and Ozanne, 2018).

MATERIALS AND METHODS

All experimental procedures were conducted according to the legal requirements of Germany and were approved by the governmental authorities of Oberbayern, Germany.

The study was carried out between March and July 2017 in a mixed forest located in the district of Starnberg, southern Germany (47°99'N, 11°39'E). One-hundred and fifty nest boxes were checked weekly starting in late March. Once a nest was completed, we visited nest boxes every other day to record the start of incubation, after which nest visits stopped. From day 10 of incubation onwards, we resumed monitoring nests every other day to record the date of hatching (day 0), while minimizing disturbance. After hatching, we randomly allocated nests to two major groups: experimental ($n=23$) and control nests ($n=10$). Experimental and control nests did not differ in mean (\pm s.e.m.) clutch size (experimental: 7.77 ± 0.29 ; control: 7.36 ± 0.41 , $t_{32}=36.30$, $P=0.44$), number of hatchlings (experimental: 6.64 ± 0.27 ; control: 6.64 ± 0.39 , $t_{32}=37.32$, $P=1.00$) or number of fledglings (experimental: 5.86 ± 0.36 ; control: 5.55 ± 0.51 , $t_{32}=18.20$, $P=0.62$). On day 5 after hatching, to exclude asynchronously hatched chicks with different growth rates, we identified the four heaviest nestlings of each brood by weighing them with a digital scale to the nearest 0.1 g (for this study, we only considered two of the four experimental nestlings, as the other two were part of a different experiment). Nestlings from the three groups did not differ in body size before the treatment (body mass $F_{2,44.48}=0.22$, $P=0.81$, $R^2_{\text{Adj}}=0.82$; tarsus length $F_{2,43.37}=1.46$, $P=0.24$, $R^2_{\text{Adj}}=0.77$). Focal chicks were randomly

marked with 1–2 yellow or white dots on the skin or feathers of the head with permanent non-toxic markers to allow for quick individual identification. Each experimental nest contained two treatment groups (one nestling per group): Cort-nestlings orally dosed daily from day 5 to day 14 with crystalline corticosterone dissolved in organic peanut oil (2 mg ml^{-1}), provided with a graduated pipet; and vehicle-nestlings that only received the oil (at the same volume as the Cort-nestlings). The two experimental nestlings in the same nest were therefore exposed to the same levels of disturbance, but differed in their exposure to exogenous corticosterone. To maintain the concentration of oral corticosterone at $0.85 \mu\text{g g}^{-1}$ of body mass throughout the nestling period, we adjusted the volume of the oral dose to nestling body mass measured on days 5, 8 and 12 (range of volumes: $2.3\text{--}6.6 \mu\text{l}$) (Fig. 1). Nestlings of control nests (control-nestlings, 4 per nest) were handled only 2 times during the nestling period (on days 5 and 15; Fig. 1) to assess the effect of disturbing the experimental nests every day. We also briefly visited control-nestlings on day 10 to refresh their colour markings. Some nestlings disappeared from their nest between one visit and the next (control, $n=3$, vehicle, $n=1$, Cort, $n=3$) while 6 nestlings in control nests lost their colour marks and were not sampled on day 15. Consequently, the final sample size was 31 control-, 22 vehicle- and 20 Cort-nestlings ($n=73$). To calculate growth rate, body mass (to the nearest 0.1 g) and tarsus length (to the nearest 1 mm) were recorded on days 5 and 15 in experimental and control nests. Growth rate was expressed as the difference between days 15 and 5 in the body mass scaled for tarsus length (Peig and Green, 2009), calculated for each measurement day (tarsus–body mass correlation on day 5: $r=0.69$, $P<0.0001$; on day 15: $r=0.70$, $P<0.0001$). Telomere length, baseline corticosterone concentration, cell metabolic traits and oxidative stress biomarkers (a full description of each parameter is given below) were measured for every chick in $80 \mu\text{l}$ of blood collected with a capillary tube on day 15 by puncturing the ulnar vein, within 3 min of opening the nest box. To minimize any variability due to daily fluctuations of

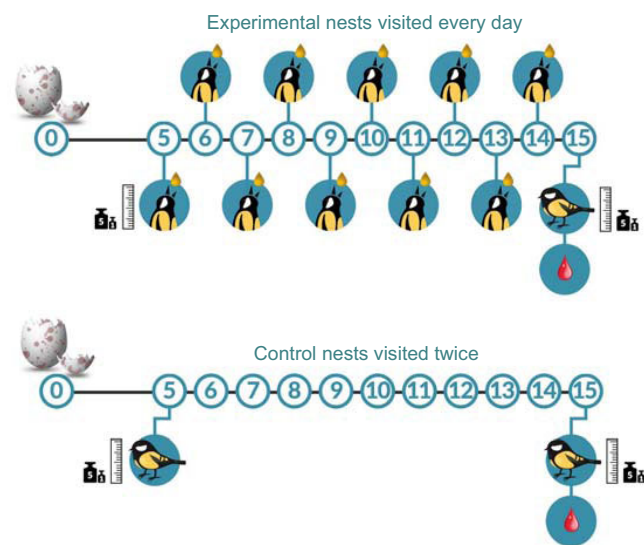


Fig. 1. Experimental design. Top: experimental nests, where nestlings were provided with an oral dose of corticosterone dissolved in oil (Cort-nestlings) or only oil (vehicle-nestlings) from post-hatching day 5 to day 14. Birds were measured on day 5 and day 15 and blood-sampled on day 15. Bottom: control nests where nestlings were handled only on day 5 and day 15 (control-nestlings) for measuring body mass, tarsus length and wing chord. Control-nestlings were also blood-sampled on day 15.

the physiological parameters, nestlings were sampled between 08:00 h and 13:00 h. Blood was immediately stored on ice and within 4 h centrifuged at 2000 *g* for 10 min; plasma was stored at -80°C and analysed within 3 months. RBCs were washed immediately to measure mitochondrial activity following Stier et al. (2017), and as described below. An aliquot of RBCs from each individual was stored in newborn calf serum (NBCS) buffer at -80°C until analysis of telomere length and gene expression.

Measurement of mitochondrial metabolism

The quantity of oxygen consumed by aerobic metabolism was measured in intact RBCs (following Stier et al., 2017), which are known to be metabolically active in birds (Stier et al., 2013; 2015). To limit contamination with leukocytes, an aliquot of 20 μl of RBCs was taken from the bottom of the tube after centrifugation (see above). RBCs were transferred into a new tube containing 1 ml of ice-cold respiratory buffer Mir05 (0.5 mmol l^{-1} EGTA, 3 mmol l^{-1} MgCl_2 , 60 mmol l^{-1} potassium lactobionate, 20 mmol l^{-1} taurine, 10 mmol l^{-1} KH_2PO_4 , 20 mmol l^{-1} Hepes, 110 mmol l^{-1} sucrose, 15 mmol l^{-1} fatty acid-free bovine serum albumin, pH 7.1). After gentle homogenization, RBCs were washed by centrifuging the samples at 500 *g* for 5 min before measurement or stored at 4°C for a time varying from 0 to 24 h until measurements. Within this time range, the duration of storage had no effect on mitochondrial measurements (metabolic rate: $F_{1,52}=0.05$, $P=0.82$; proton leak $F_{1,52}=0.68$, $P=0.42$; oxidative phosphorylation: $F_{1,52}=0.33$, $P=0.57$; maximal capacity of mitochondria: $F_{1,52}=0.02$, $P=0.89$). Immediately before the start of the mitochondrial measurements, washed RBCs were resuspended in 1 ml of Mir05 buffer already equilibrated at 37.7°C in the respirometry chamber of a Clark electrode high resolution respirometer (Oxygraph-2k, Oroboros Instruments, Innsbruck, Austria), used to quantify O_2 consumption to measure: (1) cellular metabolic rate (CMR) related to mitochondrial activity ('routine' respiration in Stier et al., 2017); (2) proton leak after inhibiting ATP-dependent O_2 consumption by oligomycin addition (1 $\mu\text{g ml}^{-1}$) ('leak' respiration in Stier et al., 2017); (3) the maximal capacity of the electron transport chain by adding the mitochondrial uncoupler carbonyl cyanide *m*-chlorophenyl hydrazine (CCCP, 1 $\mu\text{mol l}^{-1}$, titration) (electron transport system, 'ETS' in Stier et al., 2017); and (4) non-mitochondrial O_2 consumption by adding antimycin A (5 $\mu\text{mol l}^{-1}$). Non-mitochondrial respiration was used to correct all parameters described above by subtracting the quantity of O_2 recorded in this phase. All measures were normalized by the total amount of proteins quantified in an aliquot of the sample taken at the end of the metabolic measurements (Stier et al., 2017). CMR was positively correlated with proton leak ($r=0.85$, $P<0.0001$) and oxidative phosphorylation ($r=0.79$, $P<0.0001$), indicating that whenever CMR increased, the other two components increased as well. For the purpose of this study, we considered 5 metabolic variables: CMR, proton leak, oxidative phosphorylation (calculated as the difference between CMR and proton leak, the latter measured in step 2), ETS and the flux control ratio $\text{FCR}_{\text{L/R}}$ (Stier et al., 2017). $\text{FCR}_{\text{L/R}}$ is the ratio between proton leak and CMR (leak/routine) and represents the inefficiency of mitochondria in coupling respiration to the production of ATP. $\text{FCR}_{\text{L/R}}$ differs from the ratios calculated for permeabilized cells or isolated mitochondria (i.e. respiratory control ratio and phosphorous/oxygen). Using intact cells allowed us to measure cell mitochondria bioenergetics in an undisturbed cellular environment while avoiding any artefacts due to cell preparation or administration of respiratory substrates, providing more meaningful data for the purpose of our questions.

Circulating levels of corticosterone

Plasma corticosterone concentrations were determined using an enzyme immunoassay kit (cat. no. K014-H1; Corticosterone ELISA Kit, Arbor Assays) following a double diethyl ether extraction of a 10 μl plasma sample. Samples were re-dissolved in assay buffer and allowed to reconstitute overnight. A buffer blank and two stripped chicken plasma controls (with corticosterone added at concentrations of 10 and 5 ng ml^{-1} , respectively) were taken through the entire procedure. The next day, 50 μl of each sample (in duplicate) was added to individual wells on an assay plate. The inter-plate coefficient of variation (CV) was calculated as the average of the four controls on each of the five plates and was $2.35\pm 0.37\%$. The intra-plate CV was calculated as the average CV of the concentrations of all (duplicate) chick samples run on five plates and was $3.64\pm 0.31\%$. Final corticosterone concentrations were corrected for average loss during extraction, which is 15% in our lab (Baugh et al., 2014).

Expression of glucocorticoid receptor gene

We determined the expression of the gene encoding the glucocorticoid receptor (GR) in erythrocytes to confirm that the increase in proton leak observed in both vehicle- and Cort-chicks was due to the administration of corticosterone and not to the oil vehicle. This was important because fatty acids can increase membrane permeability and consequently proton leak (Echtay et al., 2002; Jastroch et al., 2010). We extracted RNA from RBC samples following the protocol described in Chiari and Galtier (2011). The analysis was run only for individuals ($n=52$) with sufficient sample volume after mitochondrial and telomere analyses; samples were stored at -80°C until RNA extraction. We mixed RBCs (approximately 2.5–5 μl) with 230 μl of TRI Reagent BD (Sigma-Aldrich) and 5 μl of 2.5 M glacial acetic acid by vortexing and allowed samples to sit at room temperature for 5 min before adding 60 μl of chloroform, followed by vigorous shaking for 15 s. We then centrifuged samples (12,000 *g*) for 15 min at 4°C , transferred the supernatant to a new tube and added an equal volume of 70% ethanol. This mixture was then applied to a RNeasy column (RNeasy Mini Kit, Qiagen), that was centrifuged (8000 *g*) for 15 s and then washed with buffers RW1 and RPE following the standard manufacturer's protocol with a final elution step in 30 μl of EB buffer. We measured RNA concentration and the A_{260}/A_{280} ratio using a Nanodrop Spectrophotometer (ND-1000) and only samples with an A_{260}/A_{280} ratio within the range 1.8–2.14 were used. For each sample, we used 400 ng of RNA as a template for cDNA synthesis using the iScript cDNA synthesis kit (Bio-Rad) in a 20 μl reaction according to the manufacturer's instructions. We diluted cDNA 1:10 before use as template in qRT-PCR assays. We designed primers for genes encoding the GR (nuclear receptor subfamily 3 group C member 1, *nr3c1*, accession no. XM_015642077.2), ubiquitin conjugating enzyme E2 D2 (*ube2d2*, accession no. XM_015641919.1) and eukaryotic translation initiation factor 3 subunit B (*eif3b*, accession no. XM_015642394.1) with NCBI Primer-BLAST (Ye et al., 2012). We ensured that each amplicon spanned at least one exon–exon boundary and when possible at least one primer within a given pair was designed to anneal across an exon–exon junction. We initially selected both *ube2d2* and *eif3b* as reference genes based on a report on the suitability of a panel of eight reference genes commonly used for quantitative PCR on whole blood and blood-derived samples (Oturai et al., 2016). Eurofins Genomics (Germany) synthesized primers; sequences along with detailed results from standard curves are listed in Table S1. We conducted

and reported all qRT-PCR assays according to guidelines by Livak and Schmittgen (2001) and Bustin et al. (2009). We ran assays on a LightCycler 480 II (Roche) machine using the SsoAdvanced Universal SYBR Green Super mix (Bio-Rad) in 384-well plates (Roche) and each reaction was run in duplicate. We performed qRT-PCR assays across four plates. Each well consisted of a 10 μ l reaction containing 1 \times SsoAdvanced Universal SYBR Green Super mix, 340 nmol l⁻¹ of each primer and 3 ng of cDNA template (i.e. 1.5 μ l of the 1:10 cDNA dilution; the estimate of template amount assumes a one-to-one correspondence between input RNA and synthesized cDNA). The cycling conditions were: pre-incubation step at 95°C for 30 s, 45 cycles at 95°C for 10 s, annealing and extension at 60°C for 30 s, with acquisition at the end of each cycle, followed by a melt curve (95°C for 5 s with 5 acquisitions per °C from 65 to 97°C with a 0.11°C ramp rate). We performed calculations from the raw amplification data using LightCycler 480 software (version 1.5.1.62) and used GraphPad Prism (version 7.05) for additional quality control analyses such as for testing for group differences on reference gene levels and calculating standard curve correlation coefficients. On every plate, we confirmed that each primer pair produced a single melt curve peak in the presence of cDNA template and showed no amplification when water was used as template. We ran a standard curve with serially diluted cDNA (1:10 to 1:1000) from a single sample to calculate the amplification efficiency of each primer pair. Efficiency was calculated with the Absolute Quantification tool and 2nd Derivative Maximum method which uses the formula $\text{Efficiency} = 10^{-1/\text{slope}}$ based on the quantification cycle [C_q, termed crossing point (C_p) in the software] and log concentration of template in each well. The theoretical efficiency of perfect amplification (i.e. exact doubling with each cycle) is 2; the efficiencies for *nr3c1*, *ube2d2* and *ef3b* were 1.987, 1.972 and 1.779, respectively. Because the efficiency for *ef3b* was well below 1.9, we deemed it not reliable and excluded it from the analysis and therefore used only *ube2d2* as a reference gene for calculating relative expression of the GR. For *nr3c1* and *ube2d2*, the correlation coefficients (r^2) from the standard curves were 0.9801 and 0.9998, respectively. We confirmed that the C_q values for *ube2d2*, pooled from all four plates, did not vary among the three treatment groups (ANOVA $F_{2,45} = 2.129$, $P = 0.1307$; C_q mean \pm s.e.m.: 19.41 \pm 0.12).

Oxidative stress

Plasma oxidative damage was quantified by measuring the levels of reactive oxygen metabolites (ROMs), hydroperoxides produced by the oxidation of lipids, proteins and nucleic acids, with the d-ROM test (Diacron International, Grosseto, Italy; Costantini et al., 2006). The d-ROM test has been shown to be a valuable assay for the quantification of oxidative stress through hydrogen peroxides and was validated by comparison with electron paramagnetic resonance in diverse biological matrixes (Costantini, 2016). The d-ROM assay was performed on 2 μ l of plasma and 100 μ l of the reactive solution provided with the kit. The absorbance was read with a microplate reader (Multiskan Go, Thermo Fisher Scientific, Vantaa, Finland) at a wavelength of 546 nm in endpoint mode. Measurements are expressed as mmol l⁻¹ of H₂O₂ equivalents. All samples, the calibrator and controls for high and low concentrations were run in duplicate. The inter-plate CV was calculated as the average concentration of the four controls on each of the six plates and was 7.83 \pm 3.2%. The intra-plate CV was calculated as the average CV of the concentrations of control samples run on six plates and was 3.18 \pm 0.74%. Plasma non-enzymatic antioxidants were quantified using the OXY-Adsorbent test (Diacron International) (Costantini et al., 2006). This assay quantifies the total antioxidant capacity of the sample exposed to the oxidative action of

hypochlorous acid (HOCl) and it was performed by using an aliquot of 2 μ l of diluted plasma, reference standards and controls for high and low concentrations (all diluted 2:50 with distilled water) or blank (i.e. only water). After incubation at 37°C with 200 μ l of HOCl solution for 10 min, 2 μ l of the chromogen provided with the kit was added to each well and the absorbance read at 546 nm with a microplate reader (Multiskan Go, Thermo Fisher Scientific). The antioxidant capacity is expressed in μ mol HOCl ml⁻¹. All samples, standards and blank were run in duplicate. The inter-plate CV was calculated as the average concentration of the four controls on each of the six plates and was 15.86 \pm 2.26%. The intra-plate CV was calculated as the average CV of the concentrations of control samples run on six plates and was 6.25 \pm 1.34%.

Telomere length

Absolute length of telomeres was measured in RBCs using a non-denaturing terminal restriction fragment (TRF) analysis following Haussmann and Vleck (2002). The measurement of RBC telomeres in birds has been validated in several studies (Haussmann et al., 2003; Heidinger et al., 2012; Bateson et al., 2015; Vedder et al., 2017). It has also been shown that RBC telomere length is positively correlated with that in several tissues such as spleen, muscle, heart, liver and brain in zebra finches (*Taeniopygia guttata*) (Reichert et al., 2013). Great tits, like certain other bird species (Delany et al., 2000), have at least two classes of telomeres: Class III ultra-long telomeres (20–240 kb) and Class II telomeres (3–20 kb; Atema et al., 2019). Class III telomeres were not examined in this study because they do not shorten with age in adults and it is not known whether they are related to fitness (Atema et al., 2019). We measured Class II telomere lengths in 5–10 μ l RBCs, diluted in 1 ml buffer (NBSC) and stored at –80°C until DNA extraction. DNA was extracted using Genra Puregene Kit (Qiagen), after first thawing the frozen samples at 37°C. Samples were centrifuged at 8000 rpm for 5 min, buffer was discarded and 10 μ l of RBCs was added to 600 μ l cell lysis solution and 10 μ l proteinase K. RBCs were digested by incubation at 56°C for 3 h, shaking it every 15 min. To remove RNA, we added 2.5 μ l RNase A solution followed by incubation at 56°C for 15 min. To facilitate protein precipitation, samples were allowed to cool down for 20 min and 230 μ l of protein precipitation solution was added. After centrifugation at 13,000 rpm for 10 min, we transferred the supernatant to a fresh tube and added 700 μ l of isopropanol. As an alternative, in the event of a possible low DNA yield, we added 0.5 μ l of glycogen solution per 300 μ l of isopropanol. Sample tubes were inverted 50 times and then centrifuged at 13,000 rpm for 10 min. The DNA pellets were washed with 600 μ l 70% ethanol, air-dried for 15–20 min and re-suspended in 25 μ l DNA rehydration solution or, in the case of a possible low DNA yield, in a smaller volume of DNA rehydration solution. Tubes were incubated at 65°C for 1 h, then shaken at low speed and room temperature overnight. Samples were restriction digested overnight prior to running them on an agarose gel with 0.5 \times TBE buffer (as described below). After overnight digestion, we added 1.5 μ l of loading dye (10 \times Bluejuice) to each sample and stored them at 4°C. For the radio-labelling of telomere oligo and 1kb+ ladder, we mixed the probes with forward rxn buffer (telomere oligo, only), exchange rxn buffer (1kb+ ladder, only), ³²P labelled γ -ATP, T4 polynucleotide kinase and water. We added each reaction to Sephadex spin columns, spun the columns down at 4000 rpm and stored labelled products at 4°C. In preparation for gel loading of samples and ladder, we prepared a 10 μ l of ladder solution per lane, consisting of 3 μ l ladder, 3 μ l loading dye (10 \times Bluejuice) and 4 μ l water. To prepare 0.8% gel, we used agarose for pulsed field

electrophoresis running gel (Sigma) and 10× TBE buffer solution (Life Technologies). After placing the gel in a Bio-Rad CHEF-DR II pulsed fields electrophoresis unit, ladders and samples were loaded and the gel was run for 19 h at 3.0 V cm⁻¹. After the run, the gel was washed with 50 ml 2× SSC buffer (Ultra Pure 20× SSC buffer Life Technologies) for 30 min, then drained by placing it in a gel dryer. To pre-hybridize the gel, we incubated it 37°C for 60 min with 50 ml hybridization solution. We then added 50 ml hybridization/oligo solution to the gel and incubated it overnight, with the same conditions as described in the previous step. The hybridization/oligo solution was prepared by adding 5 µl of labelled oligo to one vial of hybridization solution. The following day, the gel was washed 3 times with 0.25× SSC solution, dried and wrapped in cling film. Finally, the gel was placed in a phosphor screen cassette for 4 days, then visualized using a Typhoon Variable Mode Imager (Amersham Biosciences). Average telomere length was quantified by densitometry in the program ImageJ (version 2.0) within the limits of our molecular size markers (2–40 kb). All samples were run using five gels and analysis was performed singularly because of DNA quantity limitation and because this protocol showed low CV (intra-gel CV based on duplicates: 2.54%; inter-gel CV based on the repeated standard sample: 3.16%; Japanese quail, *Coturnix*

japonica; Stier et al., 2019b). In some cases, TRF did not work properly (26 samples did not contain enough DNA and in 8 samples the quality of the TRF signal was too low); therefore, results are available for 37 individuals.

Statistical analysis

We obtained data for 73 individuals. As some data were missing for some individuals (e.g. not enough blood to perform all physiological analyses, low quality of mitochondrial or telomere measurements, etc.), sample sizes differ slightly among models. For growth rate and corticosterone concentrations that each had only 6 missing values, we replaced the missing data (Nakagawa and Freckleton, 2008; Moiron et al., 2018) with least squares means predicted for each treatment group using a multivariate normal imputation model. Results with and without missing points did not substantially differ. To test for the effect of the treatment on all variables measured, we used linear mixed models with nest as a random effect to account for non-independency of siblings, and treatment as fixed factor. Whenever the random effect did not explain any variance (in two cases, i.e. GR and ROMs, the percentage of variance explained by the random factor was equal to 0, as reported in Table 1), it was removed from the model.

Table 1. Results of models run to analyse the effect of treatment on the different response variables

Variable (<i>n/R</i> _{Adj})	Fixed effect					Random effect		
	Estimate (s.e.)	d.f.	<i>F</i>	<i>P</i>	Rank/BH <i>P</i>	% Variance	Variance [nest]	Variance [residual]
Corticosterone (73/0.58)								
Intercept	0.07 (0.13)	30.83				36.70	0.32 [0.01,0.63]	0.55 [0.37,0.91]
Treatment [Cort]	0.54 (0.15)	43.29	6.33	0.004	1/0.005			
Telomere length (37/0.57)								
Intercept	0.03 (0.15)	26.78				25.47	0.19 [−0.09,0.47]	0.55 [0.32,1.15]
Treatment [Cort]	−0.67 (0.19)	29.53	5.80	0.0075	2/0.009			
FCR (52/0.48)								
Intercept	−0.007 (0.14)	26.97				23.79	0.20 [0.19,−0.18]	0.64 [0.39,1.31]
Treatment [Cort]	0.26 (0.18)	33.90	4.67	0.016	3/0.013			
Leak (52/0.41)								
Intercept	0.002 (0.14)	28.02				19.03	0.17 [−0.20,0.53]	0.70 [0.42,1.38]
Treatment [Cort]	0.49 (0.18)	34.92	4.58	0.017	4/0.018			
GR (39/0.15)								
Intercept	0.04 (0.15)	37				0	Removed	
Treatment [Cort]	0.55 (0.21)	36	4.30	0.021	5/0.023			
Growth rate (73/0.72)								
Intercept	−0.11 (0.14)	31.3				53.47	0.47 [0.13,0.81]	0.41 [0.28,0.67]
Treatment [Cort]	−0.33 (0.15)	44.4	3.13	0.051	0.027			
CMR (52/0.49)								
Intercept	0.01 (0.15)	25.58				29.89	0.28 [0.22,−0.15]	0.67 [0.39,1.37]
Treatment [Cort]	0.46 (0.18)	33.36	3.15	0.056	7/0.032			
OXY (61/0.58)								
Intercept	0.04 (0.13)	32.54				15.34	0.14 [−0.16,0.44]	0.79 [0.52,1.35]
Treatment [Cort]	0.06 (0.18)	40.81	2.70	0.079	8/0.036			
ETS (52/0.57)								
Intercept	0.02 (0.16)	27.18				38.32	0.38 [−0.07,0.83]	0.61 [0.36,1.25]
Treatment [Cort]	0.41 (0.18)	33.59	2.54	0.094	9/0.041			
OXPPOS (52/0.59)								
Intercept	0.03 (0.17)	25.86				42.29	0.43 [−0.07,0.93]	0.59 [0.34,1.26]
Treatment [Cort]	0.27 (0.18)	32.22	2.23	0.12	10/0.045			
ROMs (66/0.12)								
Intercept	0.002 (0.13)	64				0	Removed	
Treatment [Cort]	0.28 (0.31)	63	0.55	0.58	11/0.05			

Variables are ordered from higher to lower significance terms [rank reported with Benjamini–Hochberg (BH)-corrected *P*-values]. *P*-values were considered significant only when lower than *P*-values calculated according to Benjamini and Hochberg (1995). Reference treatment group is the control group; estimate values are reported only for corticosterone treatment. All analyses were performed with z-scored variables. *n*, sample size; *R*_{Adj}², *R*² adjusted for model fit; FCR, flux control ratio (proportion of proton leak to cell metabolic rate); Leak, proton leak; GR, glucocorticoid receptor; CMR, cell metabolic rate; OXY, antioxidant capacity; ETS, maximal mitochondrial capacity of the electron transport system; OXPPOS, oxidative phosphorylation; ROMs, reactive oxygen metabolites. Significant *P*-values are in bold.

To test the metabolic telomere hypothesis and investigate whether corticosterone concentration explained the variation in cell metabolic traits and telomere length at the individual level, we ran separate models for CMR and proton leak (the two metabolic traits affected by the treatment) as response variables and corticosterone concentration, treatment and their interaction as fixed factors, while nest was always retained as a random factor. The same model was run with telomere length as the response variable. A further explanatory model for telomere length to assess the effect of mitochondria trait and oxidative stress on telomeres was run by including the covariates ROMs and proton leak together with their interaction with treatment. When outliers were visible, models were run with and without them (see Results).

All analyses were performed using JMP 15 (SAS Institute Inc., Cary, NC, USA), which calculates the significance level (P -values, $\alpha=0.05$) for each fixed effect using F -statistics. In line with this approach, we analysed *post hoc* between-group differences in least square means with Student's t -test corrected for false discovery rate (FDR as explained below), which is also supported by inferential interpretation of the overlap of 95% confidence intervals (CIs) among group means visualized in all graphs (Cumming and Finch, 2005; Cummings and Mollaghan, 2006). For all models, we used z -score normalized variables. We checked whether variables met the assumptions of homogeneity of variance and normal distribution by visually analysing the graphical distributions of fitted values versus their residuals. Corticosterone, GR expression and ROMs were log transformed. To correct for multiple testing among models, we applied the Benjamini–Hochberg (BH) procedure (Benjamini and Hochberg, 1995) that controls for FDR (P -values were considered significant only when equal to or below BH P -values reported in Table 1). For *post hoc*

pairwise mean comparisons between treatments, we report only significant FDR-adjusted P -values calculated by the JMP add-in (SAS v0.07.jmpaddin). All data are given as means \pm 95% CI.

RESULTS

Corticosterone

Oral corticosterone treatment was effective in raising corticosterone levels in Cort-nestlings (which remained within the natural range for this species; Casagrande and Hau, 2018) (Table 1) but only in comparison with control-nestlings (Fig. 2A). The expression of the GR gene varied among groups (Table 1, Fig. 2B), with Cort-nestlings having higher levels of GR expression than control-nestlings (Fig. 2C). Circulating corticosterone and GR expression in vehicle-nestlings were intermediate and not different from those of Cort- or control-nestlings, perhaps owing to the daily disturbances to the vehicle-nestlings. GR expression was positively associated with baseline corticosterone concentration (Cort: $F_{1,38}=6.08$, $P=0.018$), independently of treatment (Cort \times treatment, $F_{2,37}=1.75$, $P=0.19$; treatment, $F_{2,37}=0.64$, $P=0.54$; $R^2_{\text{adj}}=0.19$, $n=39$; Fig. 3). We examined the relationship between GR expression and proton leak, finding that birds with higher relative proton leak, which accounts for the effect of CMR, had higher GR expression (FCR_{L/R}, GR: $F_{1,34}=8.78$, $P=0.006$) independently of treatment (GR \times treatment: $F_{2,33}=0.51$, $P=0.60$; treatment: $F_{2,33}=0.93$, $P=0.40$; $R^2_{\text{adj}}=0.32$, $n=35$; Fig. 3).

Telomeres

Cort-nestlings had shorter telomeres than control-nestlings (Table 1, Fig. 2C), while vehicle-nestlings showed intermediate values that did not differ from those of Cort- or control-nestlings (Fig. 2C).

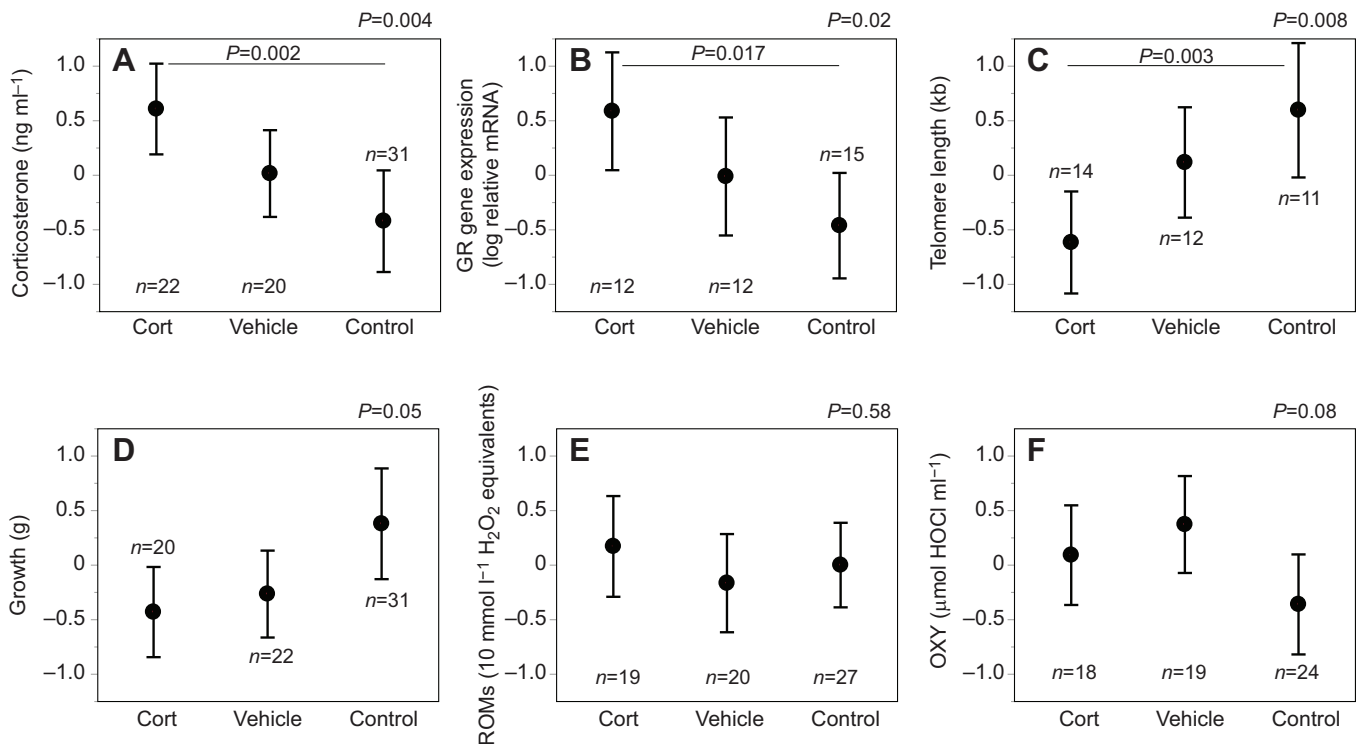


Fig. 2. Effect of corticosterone treatment on telomere length, growth and oxidative state. (A) Baseline corticosterone concentrations. (B) Expression of the glucocorticoid receptor (GR) gene. (C) Telomere length. (D) Growth rate from day 5 to day 15 (scaled by body mass). (E) Reactive oxygen metabolite (ROM) concentration (expressed as H₂O₂ equivalents). (F) Antioxidant capacity (measured by the OXY-adsorbent test and expressed in μmol HOCl neutralized per ml). Shown are group least square means with 95% confidence interval (CI). Significant P -values over bars refer to between-group *post hoc* comparisons and are false discovery rate (FDR) adjusted; P -values above each panel refer to overall model results. To simplify comparisons, variables were non-dimensionalized by z -score standardization but units of measure are retained for clarity (original values reported in Table 2).

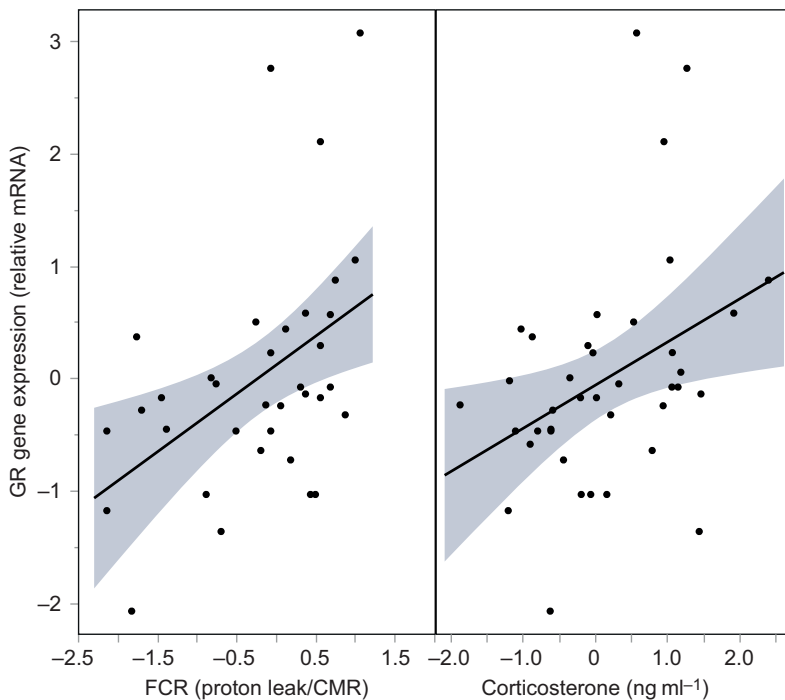


Fig. 3. Relationship of glucocorticoid receptor (GR) expression with relative proton leak and corticosterone concentration. (A) FCR. (B) Circulating corticosterone concentration. To simplify comparisons, variables were non-dimensionalized by z-score standardization but units of measure were retained for clarity.

Excluding one short telomere outlier (telomere length 10.25 kb, Cort-group; Fig. 2C) did not alter these results (treatment, $F_{2,28.07}=4.89$, $P=0.015$). This outlier was therefore retained in the next models. The effect of corticosterone on telomere length was confirmed at an individual level because higher baseline corticosterone levels were associated with shorter telomeres only in Cort-nestlings (Cort \times treatment: $F_{2,28.31}=3.35$, $P=0.049$; treatment: $F_{2,24.95}=6.88$, $P=0.004$, Cort: $F_{1,28.95}=0.02$, $P=0.89$; $\beta_{\text{Cort-nestlings}}=-0.70$, $**P<0.01$, $\beta_{\text{vehicle-nestlings}}=-0.11$; $R^2_{\text{Adj}}=0.46$, $n=37$; estimates are related to the control group). Telomere length was negatively associated with proton leak only in Cort-nestlings (proton leak \times treatment: $F_{2,16.24}=4.72$, $P=0.024$; treatment: $F_{2,12.53}=7.81$, $P=0.006$; proton leak: $F_{1,13.62}=3.39$, $P=0.09$; ROMs \times treatment: $F_{2,20.15}=2.34$, $P=0.12$; ROMs: $F_{2,20.12}=0.13$, $P=0.72$; estimate for proton leak: $\beta_{\text{Cort-nestlings}}=-0.58$, $**P<0.01$, $\beta_{\text{vehicle-nestlings}}=-0.29$; $R^2_{\text{Adj}}=0.37$, $n=30$; estimates are related to the control group).

Growth rate

Growth rate (in scaled mass index) was marginally lowered by corticosterone treatment, but the effect was not significant after correcting for multiple testing (Table 1, Fig. 2D).

Oxidative state

Corticosterone treatment did not affect nestling oxidative state, at least for the traits that we measured. Providing additional corticosterone did not affect ROM concentration (Table 1, Fig. 2E). ROMs showed three outliers despite log-transformation of the data, explaining the low fit of the model (control: $1.3 \text{ mmol l}^{-1} \text{ H}_2\text{O}_2$ equivalents; Cort: $0.4 \text{ mmol l}^{-1} \text{ H}_2\text{O}_2$ equivalents; vehicle: $1.5 \text{ mmol l}^{-1} \text{ H}_2\text{O}_2$ equivalents). Re-running the model without outliers confirmed the non-significant effect of treatment on ROMs ($F_{2,38.6}=0.79$, $P=0.46$; $R^2_{\text{Adj}}=0.32$). Treatment did not affect the antioxidant barrier (Table 1, Fig. 2F).

Mitochondrial metabolism

Corticosterone treatment affected some components of mitochondrial metabolism but not others. Cort-nestlings tended to

show higher cellular metabolic rate than vehicle- and control-nestlings (Table 1, Fig. 4A). Corticosterone treatment did not alter cell respiration linked to oxidative phosphorylation in any group ($F_{2,32.22}=2.23$, $P=0.12$; Table 1, Fig. 4B). Instead, cell respiration linked to proton leak was significantly higher in Cort- than in control-nestlings (Table 1, Fig. 4C), while that in vehicle-nestlings did not differ from values for Cort- or control-nestlings (Fig. 4C). Cort- and vehicle-nestlings had less efficient mitochondria as shown by a higher proportion of proton leak/CMR (i.e. FCR) and consequently decreased proportion of oxidative phosphorylation/CMR (Table 1, Fig. 4D) than control-nestlings. The treatments did not affect ETS (the maximal respiratory capacity of mitochondria) (Table 1, Fig. 4E).

While the effect of corticosterone on cellular metabolic rate was weak at the group level, it was highly significant when individuals were examined across all treatments; nestlings with higher baseline corticosterone concentrations had higher CMR (Cort: $F_{1,44.22}=10.96$, $P=0.002$; $\beta_{\text{Cort}}=0.48$; $R^2_{\text{Adj}}=0.70$, $n=52$), independently of treatment (Cort \times treatment: $F_{2,40.35}=1.71$, $P=0.20$; treatment: $F_{2,35.4}=0.54$, $P=0.59$). Similarly, birds with higher corticosterone concentrations had a higher proton leak independently of the treatment (Cort: $F_{1,43.87}=12.93$, $P=0.0008$; $\beta_{\text{Cort}}=0.50$; Cort \times treatment: $F_{2,39.57}=1.09$, $P=0.35$; treatment: $F_{2,34.43}=0.87$, $P=0.43$, $R^2_{\text{Adj}}=0.72$, $n=52$).

DISCUSSION

Simulating a stressful developmental environment by administering a daily dose of corticosterone to free-living great tit nestlings led to shorter telomere lengths in comparison with the control group, as expected. Our findings also revealed that elevated corticosterone concentrations decreased the efficiency of the mitochondria to produce ATP, instead probably generating heat by increasing the proton leak component of metabolic rate. Hence, the treatment affected mitochondrial metabolism, but not measures of oxidative stress. Furthermore, telomere length of nestlings was explained on an individual level by corticosterone concentration and proton leak. In particular, the models suggested a treatment-specific and dose-dependent effect of both

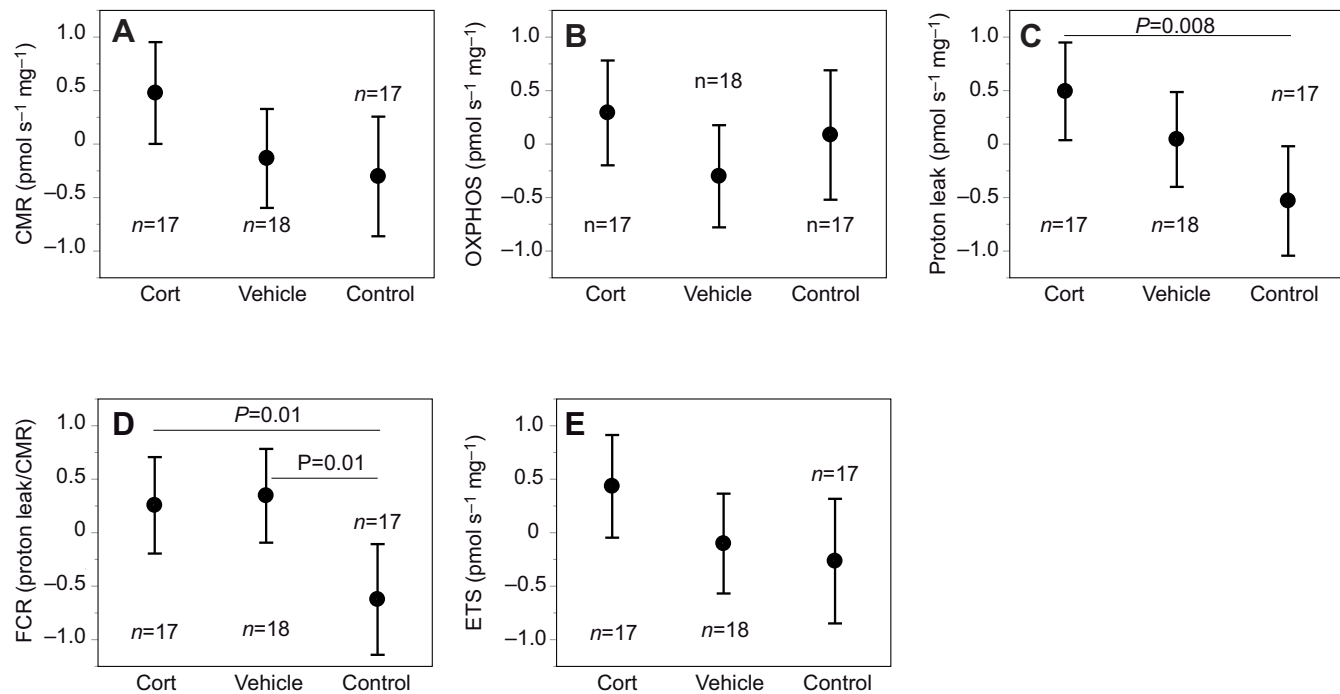


Fig. 4. Effect of corticosterone treatment on mitochondrial metabolism. (A) Mitochondrial activity (measured as cellular metabolic rate, CMR). (B) Oxidative phosphorylation (OXPHOS). (C) Proton leak. (D) Mitochondrial inefficiency (flux control ratio, FCR, the proportion of proton leak to CMR). (E) Maximal mitochondrial capacity of the electron transport system (ETS). Values in A–C and E are expressed as amount of oxygen consumed by mitochondria per unit time, normalized for the amount of blood used. Shown are group least square means with 95% CI. Significant *P*-values over bars refer to between-group *post hoc* comparisons and are FDR adjusted; *P*-values above each panel refer to overall model results. Variables were non-dimensionalized by *z*-score standardization but units of measure were retained for clarity (original values reported in Table 2).

corticosterone and proton leak on telomere length. Indeed, Cort-nestlings (which had the highest concentration of corticosterone of the three groups), showed a negative association between telomere length and, respectively, proton leak and corticosterone. Vehicle-nestlings also showed a negative relationship between telomere length and both proton leak and corticosterone. However, the slopes of these associations were not significantly different from those for control-nestlings (for corticosterone, $\beta = -0.11$; for proton leak, $\beta = -0.29$), because of the intermediate levels of corticosterone concentration, telomere length and proton leak shown by vehicle-nestlings in relation to both Cort- and control-nestlings. The opposite relationships were observed in control-nestlings, where corticosterone levels and proton leak were positively related to telomere length. These results suggest that enhanced levels of glucocorticoids can accelerate telomere attrition in RBCs during early development via changes in the cellular metabolic machinery in a dose-dependent fashion.

Mitochondria play a central role in a cell's life by producing about 90% of its energy requirements in the form of ATP through oxidative phosphorylation (Jastroch et al., 2010). Under normal conditions, about 80% of the proton gradient existing between the inter-membrane space and the matrix of a mitochondrion serves to produce ATP, while the rest is dissipated in the form of heat via the proton leak (Rolfe and Brand, 2017). One idea is that this controlled 'inefficiency' of the cell in producing ATP through the proton leak has evolved to protect the organism from the oxidative damage caused by the production of ROS (uncoupling to survive hypothesis; Brand, 2000; Bratic and Trifunovic, 2010; Stier et al., 2014a). Metabolic ROS are generated by the electrons that escape from the electron transport chain during oxidative phosphorylation

(Bottje, 2014), where a large proton gradient slows down the speed at which electrons are being processed, thereby increasing the probability of electron leakage (Brookes, 2005). Consequently, decreasing the proton gradient by releasing protons back into the mitochondrial matrix can reduce the formation of ROS. The uncoupling to survive hypothesis is still highly debated because the proton leak can have positive, negative or no effect on ROS generation (Stier et al., 2014a).

Uncouplers can downregulate the production of ATP by 35–50%, similar to the increase in proton leak that we recorded in Cort-nestlings in our experiment (Fig. 4C). Corticosterone could have actively boosted proton leak as a coping mechanism during challenging phases; for example, by increasing heat production to accelerate temperature-sensitive processes like muscle reactivity or immune function. In our study, proton leak could also have helped the developing chicks to thermoregulate (Walter and Seebacher, 2009). In addition, the glucocorticoid-induced proton leak (Fig. 4B, C) could have protected the cells from ROS production, as suggested by the uncoupling to survive hypothesis. Indeed, even though Cort-nestlings had a higher mitochondrial metabolic rate (Fig. 4A), they did not have increased ROM concentrations.

Telomere maintenance may be costly because its machinery ties up resources like nucleotides, proteins and enzymes that could be allocated to other cellular functions (Young, 2018; Casagrande and Hau, 2019). Glucocorticoids are considered to mediate life history trade-offs (Crespi et al., 2013), and telomere shortening could represent the outcome of a decision towards increased investment into current versus future survival processes under stressful conditions (Young, 2018; Casagrande and Hau, 2019), as mimicked by our corticosterone treatment. The metabolic

telomere attrition hypothesis proposes that glucocorticoid-induced telomere attrition occurs during times of severe energetic stress, when the organism needs to reduce energy-demanding anabolic processes (Casagrande and Hau, 2019). According to this hypothesis, increased telomere shortening can occur as part of the transition into an organismal emergency state induced by glucocorticoids to prioritize immediate survival over other processes. Reduced telomere maintenance then could have two functions: (1) it would make resources available that would otherwise be used for telomere maintenance (Young, 2018; Casagrande and Hau, 2019); and (2) short telomeres could serve signalling functions within the cell to re-establish energy balance and/or further influence life history decisions (Bateson and Nettle, 2018; Young, 2018; Casagrande and Hau, 2019; Giraudeau et al., 2019). This hypothesis is based on biochemical evidence that metabolic stress, as expressed by a downregulation of anabolic processes, results in telomere shortening (Ungar et al., 2011). Intriguingly, glucocorticoids can downregulate anabolic metabolism by inhibiting the cell sensor target of rapamycin (TOR; Casagrande and Hau, 2019). While our study demonstrates that corticosterone decreased mitochondrial efficiency by increasing proton leak, we did not determine whether anabolic processes were inhibited and further studies are needed in this respect. However, corticosterone treatment tended to reduce growth, suggesting indirect evidence for a downregulation of anabolic processes as new tissue generation relies on anabolic events such as protein synthesis. Growth rate tended to be reduced in vehicle-nestlings as well, but to a lesser extent than in Cort-nestlings (Fig. 2D), suggesting that anabolic processes were also inhibited in this group. A specific action of corticosterone on proton leak in early life stages could explain why the effect of glucocorticoids on telomeres is so strong during development. Because corticosterone decreases the efficiency of the mitochondria to produce ATP, which is needed for growth, Cort-nestlings tended to show a decreased growth rate. A similar scenario was also observed in vehicle-nestlings, which did not differ from Cort-nestlings in telomere length. It is possible that the marginally lower CMR of vehicle-nestlings allowed them to save resources in comparison to Cort-nestlings, but at present this is speculative and requires experimental testing. However, disentangling the effects of growth rate from telomere length was an important aim of our study. Telomere loss is often observed when growth rate is enhanced (Ringsby et al., 2015; see Introduction). In our study, Cort-nestlings had shorter telomeres and a slower growth rate in comparison to control-nestlings (Fig. 2D), indicating that the hormone did not affect telomeres through growth rate.

The experimental increase in corticosterone concentrations did not appear to alter the oxidative status of Cort-nestlings, at least not

as far as we could assess in the current study. Also, our measure of redox state did not explain telomere length. Apparently, the increased metabolic rate in Cort-nestlings was not sufficient to induce greater oxidative damage. This finding corroborates data from other wild avian species, where glucocorticoids had either no effect on oxidative stress or in some cases even a protective effect (Lendvai et al., 2014; Casagrande and Hau, 2018; Vágási et al., 2018; Vitousek et al., 2018). For example, experimentally increasing workload during nestling provisioning in male great tits enhanced circulating baseline glucocorticoids (to about 12 ng ml⁻¹, comparable to titres in the present study; Table 2), but corticosterone concentrations were not related to oxidative damage or the antioxidant barrier (Casagrande and Hau, 2018). Thus, our data do not support the idea that glucocorticoids are pro-oxidants, at least when levels remain within the natural range as in our study. However, we are aware of the limitations that are associated with measuring oxidative stress in plasma and relating it to what happens inside cells (Reichert and Stier, 2017). Thus, our conclusions have to be treated with caution for now.

Visiting the nest every day represented a disturbance as indicated by the fact that vehicle-nestlings did not differ from Cort-nestlings in any of the variables considered in the present study (Figs 2 and 4; see also Herborn et al., 2014). This could explain why vehicle-nestlings, like their corticosterone-treated siblings, showed a lower mitochondrial efficiency than control-nestlings (relative proton leak; Fig. 4D), which was related to both circulating levels of corticosterone and GR expression across treatment groups (Fig. 3). Consequently, we can exclude that the increased proton leak observed in Cort- and vehicle-nestlings was due to the fatty acids delivered through the peanut oil. Saturated and polyunsaturated fatty acids can enhance the proton permeability of the mitochondrial inner membrane, thus activating uncoupling proteins (UCPs) in mammals (Jastroch et al., 2010) or adenine nucleotide translocase (ANT) in birds (Walter and Seebacher, 2009). Although we cannot exclude that the oil used as a vehicle in our study increased proton leak, we think that this effect was minor because the two experimental groups received the same amount of peanut oil but proton leak increased within individuals in parallel with circulating corticosterone and GR expression. In addition, 50% of peanut oil is represented by monounsaturated fatty acids, which are known to decrease, rather than increase, proton leak in fish and birds (reviewed in Geisler et al., 2018).

Conclusions

Our experimental simulation of stressful developmental conditions for nestlings in the present study demonstrated the existence of connections between glucocorticoids, mitochondria and telomeres, as proposed by the metabolic telomere attrition hypothesis

Table 2. Least square means ± s.e. for each treatment group for variables considered in the study

Variable	Cort-nestlings	Vehicle-nestlings	Control-nestlings
Corticosterone (ng ml ⁻¹)	12.49±1.20	6.59±1.20	4.13±1.23
GR expression (relative mRNA level)	6.09±0.26	2.43±0.26	1.21±0.23
Telomere length (kb)	12.82±0.29	13.74±0.31	14.35±0.37
CMR (pmol s ⁻¹ mg ⁻¹)	3.60±0.32	2.76±0.31	2.54±0.37
OXPPOS (pmol s ⁻¹ mg ⁻¹)	1.96±0.19	1.51±0.18	1.80±0.23
Proton leak (pmol s ⁻¹ mg ⁻¹)	1.65±0.20	1.25±0.19	0.74±0.22
ETS (pmol s ⁻¹ mg ⁻¹)	7.76±0.82	5.92±0.80	5.36±0.97
FCR	0.44±0.04	0.46±0.03	0.30±0.04
ROMs (mmol l ⁻¹ H ₂ O ₂ equivalents)	1.58±0.37	0.90±0.37	1.19±0.35
OXY (μmol HOCl ml ⁻¹)	230.73±14.36	248.41±13.97	202.31±13.95
Growth rate (g)	7.72±0.43	8.07±0.42	9.42±0.52

(Casagrande and Hau, 2019). Indeed, corticosterone concentration explained individual differences in both metabolic efficiency and telomere length in experimental groups. In Cort- and vehicle-nestlings, elevated corticosterone concentration and proton leak were negatively related to telomere length, while in control-nestlings high corticosterone concentration and high proton leak were positively associated with telomere length. These findings suggest that the nature of the interactions between glucocorticoids, telomeres and mitochondria is dose dependent. Dose dependency is a well-known characteristic of glucocorticoid actions (Sapolsky et al., 2000). The present study also suggests that telomere dynamics can be associated with the energetic state of a cell and supports the suggestion that telomeres are costly to maintain. One possibility is that proton leak negatively affected telomeres only in Cort-nestlings because this was the only group that tended to have high CMR (thus a greater allocation of resources to the mitochondrial machinery that was not accompanied by a sufficient gain in ATP production, which is necessary to support telomere maintenance). In general, our findings support the view of an active regulation of telomere length during times of increased energetic needs as advocated by the metabolic telomere attrition hypothesis (Casagrande and Hau, 2019). Further investigations are needed to understand the fitness implications of this metabolic regulation of telomeres, e.g. for survival, recruitment and reproduction, in both developing and adult individuals.

Acknowledgements

We thank all the Evolutionary Physiology group for helping in different ways during the study, especially Caro Deimel for logistic support and Julia Slezacek for helping with the extraction of DNA. We are grateful to two anonymous reviewers for providing valuable comments on a previous version of the manuscript and to Alessandro Candelari for his graphic contribution to Fig. 1.

Competing interests

The authors declare no competing or financial interests.

Author contributions

Conceptualization: S.C., M.H.; Methodology: S.C., A.S., P.M., W.B., J.L., S.L., R.T.; Validation: A.S., P.M.; Formal analysis: S.C.; Investigation: S.C.; Data curation: S.C.; Writing - original draft: S.C.; Writing - review & editing: S.C., A.S., P.M., W.B., J.L., S.L., R.T., M.H.; Visualization: S.C.; Supervision: S.C., M.H.; Project administration: S.C., M.H.; Funding acquisition: S.C., M.H.

Funding

We are grateful to the Max Planck Society (Max-Planck-Gesellschaft) and the German Science Foundation (Deutsche Forschungsgemeinschaft grant CA 1789/1-1-2017) for supporting our work.

Supplementary information

Supplementary information available online at <https://jeb.biologists.org/lookup/doi/10.1242/jeb.222513.supplemental>

Data availability

Data are available from the Dryad digital repository (Casagrande et al., 2020): [dryad.cvdncjt1g](https://doi.org/10.5061/dryad.cvdncjt1g)

References

- Angelier, F., Costantini, D., Blévin, P. and Chastel, O. (2018). Do glucocorticoids mediate the link between environmental conditions and telomere dynamics in wild vertebrates? A review. *Gen. Comp. Endocrinol.* **256**, 99-111. doi:10.1016/j.ygcen.2017.07.007
- Atema, E., Mulder, E., Van Noordwijk, A. J. and Verhulst, S. (2019). Ultra-long telomeres shorten with age in nestling great tits but are static in adults and mask attrition of short telomeres. *Mol. Ecol. Resour.* **19**: 648-658. doi:10.1111/1755-0998.12996
- Bateson, M. and Nettle, D. (2018). Why are there associations between telomere length and behaviour? *Phil. Trans. R. Soc.* **373**, 20160438. doi:10.1098/rstb.2016.0438
- Bateson, M., Briol, B. O., Gillespie, R., Monaghan, P. and Nettle, D. (2015). Developmental telomere attrition predicts impulsive decision-making in adult starlings. *Proc. Biol. Sci.* **282**, 20142140. doi:10.1098/rspb.2014.2140
- Baugh, A. T., Oers, K., van Dingemans, N. J. and Hau, M. (2014). Baseline and stress-induced glucocorticoid concentrations are not repeatable but covary within individual great tits (*Parus major*). *Gen. Comp. Endocrinol.* **208**, 154-163. doi:10.1016/j.ygcen.2014.08.014
- Benjamini, Y. and Hochberg, Y. (1995). Controlling the false discovery rate: A practical and powerful approach to multiple testing. *J.R. Stat. Soc.* **57**, 289-300. doi:10.1111/j.2517-6161.1995.tb02031.x
- Bernardes de Jesus, B., Vera, E., Schneeberger, K., Tejera, A. M., Ayuso, E., Bosch, F. and Blasco, M. (2012). Telomerase gene therapy in adult and old mice delays aging and increases longevity without increasing cancer. *EMBO Mol. Med.* **4**, 691-704. doi:10.1002/emmm.201200245
- Bize, P., Criscuolo, F., Metcalfe, N. B., Nasir, L. and Monaghan, P. (2009). Telomere dynamics rather than age predict life expectancy in the wild. *Proc. R. Soc. B* **276**, 1679-1683. doi:10.1098/rspb.2008.1817
- Blackburn, E. H. and Epel, E. S. (2012). Telomeres and adversity: Too toxic to ignore. *Nature* **490**, 169-171. doi:10.1038/490169a
- Blackburn, E. H., Epel, E. S. and Lin, J. (2015). Human telomere biology: A contributory and interactive factor in aging, disease risks, and protection. *Science* **350**, 1193-1198. doi:10.1126/science.aab3389
- Boonekamp, J. J., Mulder, G., Salomons, H. M., Dijkstra, C. and Verhulst, S. (2014). Nestling telomere shortening, but not telomere length, reflects developmental stress and predicts survival in wild birds. *Proc. R. Soc. B* **281**, 20133287. doi:10.1098/rspb.2013.3287
- Boonekamp, J. J., Bauch, C., Mulder, E. and Verhulst, S. (2017). Does oxidative stress shorten telomeres? *Biol. Lett.* **13**, 20170164. doi:10.1098/rsbl.2017.0164
- Bottje, W. (2014). *Mitochondrial Physiology*, 6th edn (C. G. Scanes, (ed.)). Academic Press as an imprint of Elsevier, London.
- Brand, M. D. (2000). Uncoupling to survive? The role of mitochondrial inefficiency in ageing. *Exp. Gerontol.* **35**, 811-820. doi:10.1016/S0531-5565(00)00135-2
- Bratic, I. and Trifunovic, A. (2010). Mitochondrial energy metabolism and ageing. *Biochim. Biophys. Acta* **1797**, 961-967. doi:10.1016/j.bbabi.2010.01.004
- Brookes, P. S. (2005). Mitochondrial H⁺ leak and ROS generation: An odd couple. *Free Radic. Biol. Med.* **38**, 12-23. doi:10.1016/j.freeradbiomed.2004.10.016
- Bustin, S. A., Benes, V., Garson, J. A., Hellemans, J., Huggett, J., Kubista, M., Mueller, R., Nolan, T., Pfaffl, M. W., Shipley, G. L. et al. (2009). The MIQE guidelines: minimum information for publication of quantitative real-time PCR experiments. *Clin. Chem.* **55**, 611-622. doi:10.1373/clinchem.2008.112797
- Carroll, J. E., Cole, S. W., Seeman, T. E., Breen, E. C., Witarama, T., Arevalo, J. M. G., Ma, J. Irwin, M. R. (2016). Partial sleep deprivation activates the DNA damage response (DDR) and the senescence-associated secretory phenotype (SASP) in aged adult humans. *Brain Behav. Immun.* **51**, 223-229. doi:10.1016/j.bbi.2015.08.024
- Casagrande, S. and Hau, M. (2018). Enzymatic antioxidants but not baseline glucocorticoids mediate the reproduction-survival trade-off in a wild bird. *Proc. R. Soc. B* **285**, 20182141. doi:10.1098/rspb.2018.2141
- Casagrande, S. and Hau, M. (2019). Telomere attrition: metabolic regulation and signalling function? *Biol. Lett.* **15**, 20180885. doi:10.1098/rsbl.2018.0885
- Casagrande, S., Stier, A., Monaghan, P., Loveland, J. L., Boner, W., Lupi, S., Trevisi, R. and Hau, M. (2020). Data from Increased glucocorticoid concentrations in early life cause mitochondrial inefficiency and short telomeres. *Dryad*. <https://doi.org/10.5061/dryad.cvdncjt1g>
- Chang, A. C. Y., Ong, S.-G., LaGory, E. L., Kraft, P. E., Giaccia, A. J., Wu, J. C. and Blau, H. M. (2016). Telomere shortening and metabolic compromise underlie dystrophic cardiomyopathy. *Proc. Natl. Acad. Sci. U.S.A.* **113**, 13120-13125. doi:10.1073/pnas.1615340113
- Chiari, Y. and Galtier, N. (2011). RNA extraction from sauropsids blood: evaluation and improvement of methods. *Amphib-Reptilia* **32**, 136-139. doi:10.1163/017353710X543010
- Costantini, D. (2016). Oxidative stress ecology and the d-ROMs test: facts, misfacts and an appraisal of a decade's work. *Behav. Ecol. Sociobiol.* **70**, 809-820. doi:10.1007/s00265-016-2091-5
- Costantini, D., Casagrande, S., De Filippis, S., Brambilla, G., Fanfani, A., Tagliavini, J. and Dell'Omo, G. (2006). Correlates of oxidative stress in wild kestrel nestlings (*Falco tinnunculus*). *J. Comp. Physiol. B Biochem. Syst. Environ. Physiol.* **176**, 329-337. doi:10.1007/s00360-005-0055-6
- Costantini, D., Marasco, V. and Møller, A. P. (2011). A meta-analysis of glucocorticoids as modulators of oxidative stress in vertebrates. *J. Comp. Physiol. B Biochem. Syst. Environ. Physiol.* **181**, 447-456. doi:10.1007/s00360-011-0566-2
- Crespi, E. J., Williams, T. D., Jessop, T. S. and Delehanty, B. (2013). Life history and the ecology of stress: How do glucocorticoid hormones influence life-history variation in animals? *Funct. Ecol.* **27**, 93-106. doi:10.1111/1365-2435.12009
- Cumming, G. and Finch, S. (2005). Inference by eye confidence intervals and how to read pictures of data. *Am. Psychol.* **60**, 170-180. doi:10.1037/0003-066X.60.2.170
- Cummings, M. and Mollaghan, D. (2006). Repeatability and consistency of female preference behaviours in a northern swordtail, *Xiphophorus nigrensis*. *Anim. Behav.* **72**, 217-224. doi:10.1016/j.anbehav.2006.01.009

- de Jesus, B. B., Schneeberger, K., Vera, E., Tejera, A., Harley, C. B. and Blasco, M. A. (2011). The telomerase activator TA-65 elongates short telomeres and increases health span of adult/old mice without increasing cancer incidence. *Aging Cell* **10**, 604-621. doi:10.1111/j.1474-9726.2011.00700.x
- Delany, M. E., Krupkin, A. B. and Miller, M. M. (2000). Organization of telomere sequences in birds: evidence for arrays of extreme length and for in vivo shortening. *Cytogenet. Genome Res.* **90**, 139-145. doi:10.1159/000015649
- Eastwood, J. R., Hall, M. L., Teunissen, N., Kingma, S. A., Hidalgo Aranzamendi, N., Fan, M., Roast, M., Verhulst, S. and Peters, A. (2018). Early-life telomere length predicts lifespan and lifetime reproductive success in a wild bird. *Mol. Ecol.* **28**, 1127-1137. doi:10.1111/mec.15002
- Echtay, K. S., Roussel, D., St-pierre, J., Jekabsons, M. B., Cadenas, S., Stuart, J. A., Harper, J. A., Roebuck, S. J., Morrison, A., Pickering, S. et al. (2002). Superoxide activates mitochondrial uncoupling proteins. *Nature* **415**, 96-99. doi:10.1038/415096a
- Eisner, V., Picard, M. and Hajnóczky, G. (2018). Mitochondrial dynamics in adaptive and maladaptive cellular stress responses. *Nat. Cell Biol.* **20**, 755-765. doi:10.1038/s41556-018-0133-0
- Geiger, S., Le Vaillant, M., Lebard, T., Reichert, S., Stier, A., Le Maho, Y. and Criscuolo, F. (2012). Catching-up but telomere loss: Half-opening the black box of growth and ageing trade-off in wild king penguin chicks. *Mol. Ecol.* **21**, 1500-1510. doi:10.1111/j.1365-294X.2011.05331.x
- Geisler, C. E., Kentch, K. P. and Renquist, B. J. (2018). Non-mammalian vertebrates: distinct models to assess the role of ion gradients in energy expenditure. *Front. Endocrinol.* **8**, 224. doi:10.3389/fendo.2017.00224
- Giraudeau, M., Angelier, F. and Sepp, T. (2019). Do telomeres influence pace-of-life-strategies in response to environmental conditions over a lifetime and between generations? *BioEssays* **41**, 1800162. doi:10.1002/bies.201800162
- Glazier, D. S. (2015). Is metabolic rate a universal "pacemaker" for biological processes? *Biol. Rev.* **90**, 377-407.
- Guha, M., Srinivasan, S., Bradley Johnson, F., Ruthel, G., Guja, K., Garcia-Diaz, M., Kaufman, B. A., Rebecca Glineburg, M., Fang, J., Nakagawa, H. et al. (2018). HnRNPA2 mediated acetylation reduces telomere length in response to mitochondrial dysfunction. *PLoS ONE* **13**, 1-21. doi:10.1371/journal.pone.0206897
- Hau, M., Casagrande, S., Ouyang, J. Q. and Baugh, A. T. (2016). Glucocorticoid-mediated phenotypes in vertebrates: Multilevel variation and evolution. In *Advances in the Study of Behavior* (M. Naguib, J. C. Mitani, L. W. Simmons, L. Barrett, S. Healy and M. Zuk (eds)). Academic Press, pp. 41-115.
- Hau, M., Greives, T. J., Haussmann, M. F., Matlack, C., Costantini, D., Quetting, M., Adelman, J. S. and Partecke, J. (2015). Repeated stressor increase the rate of biological ageing. *Front. Zool.* **12**, 1-10. doi:10.1186/s12983-014-0093-6
- Haussmann, M. F. and Heidinger, B. J. (2015). Telomere dynamics may link stress exposure and ageing across generations. *Biol. Lett.* **11**, 20150396. doi:10.1098/rsbl.2015.0396
- Haussmann, M. F. and Marchetto, N. M. (2010). Telomeres: Linking stress and survival, ecology and evolution. *Curr. Zool.* **56**, 714-727. doi:10.1093/czoolo/56.6.714
- Haussmann, M. F. and Vleck, C. M. (2002). Telomere length provides a new technique for aging animals. *Oecologia* **130**, 325-328. doi:10.1007/s00442-001-0827-y
- Haussmann, M. F., Winkler, D. W., O'Reilly, K. M., Huntington, C. E., Nisbet, I. C. T. and Vleck, C. M. (2003). Telomeres shorten more slowly in long-lived birds and mammals than in short-lived ones. *Proc. Biol. Sci.* **270**, 1387-1392. doi:10.1098/rspb.2003.2385
- Haussmann, M. F., Longenecker, A. S., Marchetto, N. M., Juliano, S. A. and Bowden, R. M. (2012). Embryonic exposure to corticosterone modifies the juvenile stress response, oxidative stress and telomere length. *Proc. Biol. Sci.* **279**, 1447-1456. doi:10.1098/rspb.2011.1913
- Heidinger, B. J., Blount, J. D., Boner, W., Griffiths, K., Metcalfe, N. B. and Monaghan, P. (2012). Telomere length in early life predicts lifespan. *Proc. Natl. Acad. Sci. U. S. A.* **109**, 1743-1748. doi:10.1073/pnas.1113306109
- Herborn, K. A., Heidinger, B. J., Boner, W., Noguera, J. C., Adam, A., Daunt, F. and Monaghan, P. (2014). Stress exposure in early post-natal life reduces telomere length: an experimental demonstration in a long-lived seabird. *Proc. Biol. Sci.* **281**, 20133151. doi:10.1098/rspb.2013.3151
- Jastroch, M., Divakaruni, A. S., Mookerjee, S., Treberg, J. R. and Brand, M. D. (2010). Mitochondrial proton and electron leaks. *Essays Biochem.* **47**, 53-67. doi:10.1042/bse0470053
- Jimeno, B., Hau, M. and Verhulst, S. (2018). Corticosterone levels reflect variation in metabolic rate, independent of 'stress'. *Sci. Rep.* **8**, 1-8. doi:10.1038/s41598-018-31258-z
- Jimeno, B., Hau, M. and Verhulst, S. (2017). Strong association between corticosterone and temperature dependent metabolic rate in individual zebra finches. *J. Exp. Biol.* **220**, 4426-4431. doi:10.1242/jeb.166124
- Koch, R. E., Josefson, C. C. and Hill, G. E. (2017). Mitochondrial function, ornamentation, and immunocompetence. *Biol. Rev.* **92**, 1459-1474. doi:10.1111/brv.12291
- Kotrschal, A., Ilmonen, P. and Penn, D. J. (2007). Stress impacts telomere dynamics. *Biol. Lett.* **3**, 128-130. doi:10.1098/rsbl.2006.0594
- Lattin, C. R. and Romero, L. M. (2014). Chronic stress alters concentrations of corticosterone receptors in a tissue-specific manner in wild house sparrows (*Passer domesticus*). *J. Exp. Biol.* **217**, 2601-2608. doi:10.1242/jeb.103788
- Lendvai, A. Z., Ouyang, J. Q., Schoenle, L. A., Fasanello, V., Haussmann, M. F., Bonier, F. and Moore, I. (2014). Experimental food restriction reveals individual differences in corticosterone reaction norms with no oxidative costs. *PLoS ONE* **9**, e110564. doi:10.1371/journal.pone.0110564
- Livak, K. J. and Schmittgen, T. D. (2001). Analysis of Relative Gene Expression Data Using Real-Time Quantitative PCR and the 2^{-ΔΔCT} Method. *Methods* **25**, 402-408. doi:10.1006/meth.2001.1262
- López-Otín, C., Blasco, M. A., Partridge, L., Serrano, M. and Kroemer, G. (2013). The hallmarks of aging. *Cell* **153**, 1194-1217. doi:10.1016/j.cell.2013.05.039
- Manoli, I., Alessi, S., Blackman, M. R., Su, Y. A., Rennert, O. M. and Chrousos, G. P. (2007). Mitochondria as key components of the stress response. *Trends Endocrinol. Metab.* **18**, 190-198. doi:10.1016/j.tem.2007.04.004
- Meitern, R., Andreson, R. and Hörak, P. (2014). Profile of whole blood gene expression following immune stimulation in a wild passerine. *BMC Genomics* **15**, 1-10. doi:10.1186/1471-2164-15-533
- Moiron, M., Mathot, K. J. and Dingemans, N. J. (2018). To eat and not be eaten: Diurnal mass gain and foraging strategies in wintering great tits. *Proc. R. Soc. B* **285**, 20172868. doi:10.1098/rspb.2017.2868
- Monaghan, P. (2008). Early growth conditions, phenotypic development and environmental change. *Philos. Trans. R. Soc. London B Biol. Sci.* **363**, 1635-1645. doi:10.1098/rstb.2007.0011
- Monaghan, P. (2010). Telomeres and life histories: The long and the short of it. *Ann. N. Y. Acad. Sci.* **1206**, 130-142. doi:10.1111/j.1749-6632.2010.05705.x
- Monaghan, P. (2014). Organismal stress, telomeres and life histories. *J. Exp. Biol.* **217**, 57-66. doi:10.1242/jeb.090043
- Monaghan, P. and Haussmann, M. F. (2006). Do telomere dynamics link lifestyle and lifespan? *Trends Ecol. Evol.* **21**, 47-53. doi:10.1016/j.tree.2005.11.007
- Monaghan, P. and Haussmann, M. F. (2015). The positive and negative consequences of stressors during early life. *Early Hum. Dev.* **91**, 643-647. doi:10.1016/j.earlhumdev.2015.08.008
- Monaghan, P. and Ozanne, S. E. (2018). Somatic growth and telomere dynamics in vertebrates: relationships, mechanisms and consequences. *Philos. Trans. R. Soc. B* **373**, 20160446. doi:10.1098/rstb.2016.0446
- Muñoz-Lorente, M. A., Cano-Martin, A. C. and Blasco, M. A. (2019). Mice with hyper-long telomeres show less metabolic aging and longer lifespans. *Nat. Commun.* **10**, 1-14. doi:10.1038/s41467-019-12664-x
- Nakagawa, S. and Freckleton, R. P. (2008). Missing inaction: the dangers of ignoring missing data. *Trends Ecol. Evol.* **23**, 592-596. doi:10.1016/j.tree.2008.06.014
- Nettle, D., Monaghan, P., Gillespie, R., Briot, B., Bedford, T. and Bateson, M. (2015). An experimental demonstration that early-life competitive disadvantage accelerates telomere loss. *Proc. R. Soc. B* **282**, 20141610. doi:10.1098/rspb.2015.1005
- Oturai, D. B., Søndergaard, H. B., Börnsen, L., Sellebjerg, F. and Romme Christensen, J. (2016). Identification of suitable reference genes for peripheral blood mononuclear cell subset studies in multiple sclerosis. *Scand. J. Immunol.* **83**, 72-80. doi:10.1111/sji.12391
- Passos, J. F., Saretzki, G. and Von Zglinicki, T. (2007). DNA damage in telomeres and mitochondria during cellular senescence: Is there a connection? *Nucleic Acids Res.* **35**, 7505-7513. doi:10.1093/nar/gkm893
- Peig, J. and Green, A. J. (2009). New perspectives for estimating body condition from mass/length data: The scaled mass index as an alternative method. *Oikos* **118**, 1883-1891. doi:10.1111/j.1600-0706.2009.17643.x
- Picard, M., McEwen, B. S., Epel, E. S. and Sandi, C. (2018). An energetic view of stress: Focus on mitochondria. *Front. Neuroendocrinol.* **49**, 72-85. doi:10.1016/j.yfrne.2018.01.001
- Psarra, A. M. G. and Sekeris, C. E. (2009). Glucocorticoid receptors and other nuclear transcription factors in mitochondria and possible functions. *Biochim. Biophys. Acta Bioenergy* **1787**, 431-436. doi:10.1016/j.bbabi.2008.11.011
- Quirici, V., Guerrero, C. J., Krause, J. S., Wingfield, J. C. and Vásquez, R. A. (2016). The relationship of telomere length to baseline corticosterone levels in nestlings of an altricial passerine bird in natural populations. *Front. Zool.* **13**, 1. doi:10.1186/s12983-016-0133-5
- Reichert, S. and Stier, A. (2017). Does oxidative stress shorten telomeres *in vivo*? A review. *Biol. Lett.* **13**, 20170463. doi:10.1098/rsbl.2017.0463
- Reichert, S., Criscuolo, F., Verinaud, E., Zahn, S. and Masméjan, S. (2013). Telomere length correlations among somatic tissues in adult zebra finches. *PLoS ONE* **8**.
- Ringsby, T. H., Jensen, H., Pärn, H., Kvalnes, T., Boner, W., Gillespie, R., Holand, H., Hagen, I. J., Rønning, B., Saether, B.-E. et al. (2015). On being the right size: increased body size is associated with reduced telomere length under natural conditions. *Proc. R. Soc. B* **282**, 20152331. doi:10.1098/rspb.2015.2331
- Rolle, D. F. and Brand, M. D. (2017). Contribution of mitochondrial proton leak to skeletal muscle respiration and to standard metabolic rate. *Am. J. Physiol. Physiol.* **271**, C1380-C1389. doi:10.1152/ajpcell.1996.271.4.C1380
- Romano, G. H., Harari, Y., Yehuda, T., Podhorzer, A., Rubinstein, L., Shamir, R., Gottlieb, A., Silberberg, Y., Pe'er, D., Ruppin, E. et al. (2013). Environmental

- Stresses Disrupt Telomere Length Homeostasis. *PLoS Genet.* **9**, e1003721. doi:10.1371/journal.pgen.1003721
- Romero, L. M. (2004). Physiological stress in ecology: Lessons from biomedical research. *Trends Ecol. Evol.* **19**, 249-255. doi:10.1016/j.tree.2004.03.008
- Romero, L. M. and Wingfield, J. (2016). *Tempests, Poxes, Predators, and People* (L. M. Romero and J. Wingfield (eds)). Oxford University Press, New York.
- Roussel, D., Dumas, J. F., Augeraud, A., Douay, O., Foussard, F., Malthiery, Y., Simard, G. and Ritz, P. (2003). Dexamethasone treatment specifically increases the basal proton conductance of rat liver mitochondria. *FEBS Lett.* **541**, 75-79. doi:10.1016/S0014-5793(03)00307-7
- Sahin, E. and DePinho, R. A. (2012). Axis of ageing: telomeres, p53 and mitochondria. *Nat. Rev. Mol. Cell Biol.* **13**, 397-404. doi:10.1038/nrm3352
- Salin, K., Auer, S. K., Rudolf, A. M., Anderson, G. J., Cairns, A. G., Mullen, W., Hartley, R. C., Selman, C. and Metcalfe, N. B. (2015). Individuals with higher metabolic rates have lower levels of reactive oxygen species in vivo. *Biol. Lett.* **11**, 20150538. doi:10.1098/rsbl.2015.0538
- Sapolsky, R. M., Romero, L. M. and Munck, A. U. (2000). How do glucocorticoids influence stress responses? Integrating permissive, suppressive, stimulatory, and preparative actions. *Endocr. Rev.* **21**, 55-89. doi:10.1210/er.21.1.55
- Schultner, J., Moe, B., Chastel, O., Bech, C. and Kitaysky, A. S. (2014). Migration and stress during reproduction govern telomere dynamics in a seabird. *Biol. Lett.* **10**, 20130889. doi:10.1098/rsbl.2013.0889
- Spencer, K. A. and Verhulst, S. (2007). Delayed behavioral effects of postnatal exposure to corticosterone in the zebra finch (*Taeniopygia guttata*). *Horm. Behav.* **51**, 273-280. doi:10.1016/j.yhbeh.2006.11.001
- Spencer, K. A. and Verhulst, S. (2008). Post-natal exposure to corticosterone affects standard metabolic rate in the zebra finch (*Taeniopygia guttata*). *Gen. Comp. Endocrinol.* **159**, 250-256. doi:10.1016/j.ygcen.2008.09.007
- Stier, A., Bize, P., Schull, Q., Zoll, J., Singh, F., Geny, B., Gros, F., Royer, C., Massemin, S. and Criscuolo, F. (2013). Avian erythrocytes have functional mitochondria, opening novel perspectives for birds as animal models in the study of ageing. *Front. Zool.* **10**, 33. doi:10.1186/1742-9994-10-33
- Stier, A., Bize, P., Roussel, D., Schull, Q., Massemin, S. and Criscuolo, F. (2014a). Mitochondrial uncoupling as a regulator of life-history trajectories in birds: an experimental study in the zebra finch. *J. Exp. Biol.* **217**, 3579-3589. doi:10.1242/jeb.103945
- Stier, A., Viblanc, V. A., Massemin-Challet, S., Handrich, Y., Zahn, S., Rojas, E. R., Saraux, C., Le Vaillant, M., Prud'homme, O., Grosbelle, E. et al. (2014b). Starting with a handicap: Phenotypic differences between early- and late-born king penguin chicks and their survival correlates. *Funct. Ecol.* **28**, 601-611. doi:10.1111/1365-2435.12204
- Stier, A., Reichert, S., Criscuolo, F. and Bize, P. (2015). Red blood cells open promising avenues for longitudinal studies of ageing in laboratory, non-model and wild animals. *Exp. Gerontol.* **71**, 118-134. doi:10.1016/j.exger.2015.09.001
- Stier, A., Romestaing, C., Schull, Q., Lefol, E., Robin, J.-P., Roussel, D. and Bize, P. (2017). How to measure mitochondrial function in birds using red blood cells: a case study in the king penguin and perspectives in ecology and evolution. *Methods Ecol. Evol.* **8**, 1172-1182. doi:10.1111/2041-210X.12724
- Stier, A., Bize, P., Hsu, B.-Y. and Ruuskanen, S. (2019a). Plastic but repeatable: rapid adjustments of mitochondrial function and density during reproduction in a wild bird species. *Biol. Lett.* **15**, 9-13. doi:10.1098/rsbl.2019.0536
- Stier, A., Metcalfe, N. B. and Monaghan, P. (2019b). Ageing before birth: pace and stability of prenatal growth affect telomere dynamics. *bioRxiv*, doi:10.1101/809087
- Stier, A., Schull, Q., Bize, P., Lefol, E., Haussmann, M. and Roussel, D. (2019c). Oxidative stress and mitochondrial responses to stress exposure suggest that king penguins are naturally equipped to resist stress. *Sci. Rep.* **9**, 8545. doi:10.1038/s41598-019-44990-x
- Tissier, M. L., Williams, T. D. and Criscuolo, F. (2014). Maternal effects underlie ageing costs of growth in the zebra finch (*Taeniopygia guttata*). *PLoS One* **9**, e97705. doi:10.1371/journal.pone.0097705
- Ungar, L., Harari, Y., Toren, A. and Kupiec, M. (2011). Tor complex 1 controls telomere length by affecting the level of Ku. *Curr. Biol.* **21**, 2115-2120. doi:10.1016/j.cub.2011.11.024
- Vágási, C. I., Pătraș, L., Pap, P. L., Vincze, O., Mureșan, C., Németh, J. and Lendvai, A. Z. (2018). Experimental increase in baseline corticosterone level reduces oxidative damage and enhances innate immune response. *PLoS ONE* **13**, 1-17. doi:10.1371/journal.pone.0192701
- Varela, E., Muñoz-Lorente, M. A., Tejera, A. M., Ortega, S. and Blasco, M. A. (2016). Generation of mice with longer and better preserved telomeres in the absence of genetic manipulations. *Nat. Commun.* **7**, 11739. doi:10.1038/ncomms11739
- Vedder, O., Verhulst, S., Bauch, C. and Bouwhuis, S. (2017). Telomere attrition and growth: a life-history framework and case study in common terns. *J. Evol. Biol.* **30**, 1409-1419. doi:10.1111/jeb.13119
- Vitousek, M. N., Taff, C. C., Ardia, D. R., Stedman, J. M., Zimmer, C., Salzman, T. C. and Winkler, D. W. (2018). The lingering impact of stress: brief acute glucocorticoid exposure has sustained, dose-dependent effects on reproduction. *Proc. R. Soc. B* **285**, 20180722. doi:10.1098/rspb.2018.0722
- Von Zglinicki, T. (2002). Oxidative stress shortens telomeres. *Trends Biochem. Sci.* **27**, 339-344. doi:10.1016/S0968-0004(02)02110-2
- Von Zglinicki, T., Pilger, R. and Sitt, N. (2000). Accumulation of single-strand breaks is the major cause of telomere shortening in human fibroblasts. *Free Radic. Biol. Med.* **28**, 64-74. doi:10.1016/S0891-5849(99)00207-5
- Walter, I. and Seebacher, F. (2009). Endothelium in birds: underlying molecular mechanisms. *J. Exp. Biol.* **212**, 2328-2336. doi:10.1242/jeb.029009
- Wang, Q., Pujol-Canadell, M., Taveras, M., Garty, G., Perrier, J., Bueno-Beti, C., Shuryak, I., Brenner, D. J. and Turner, H. C. (2020). DNA damage response in peripheral mouse blood leukocytes in vivo after variable, low-dose rate exposure. *Radiat. Environ. Biophys.* **59**, 89-98. doi:10.1007/s00411-019-00825-x
- Whittemore, K., Vera, E., Martínez-Navado, E., Sanpera, C. and Blasco, M. A. (2019). Telomere shortening rate predicts species life span. *Proc. Natl. Acad. Sci. USA* **119**, 15122-15127. doi:10.1073/pnas.1902452116
- Wood, E. M. and Young, A. J. (2019). Telomere attrition predicts reduced survival in a wild social bird, but short telomeres do not. *Mol. Ecol.* **28**, 3669-3680. doi:10.1111/mec.15181
- Ye, J., Coulouris, G., Zaretskaya, I., Cutcutache, I., Rozen, S. and Madden, T. L. (2012). Primer-BLAST: A tool to design target-specific primers for polymerase chain reaction. *BMC Bioinformatics* **13**, 134. doi:10.1186/1471-2105-13-134
- Ye, J., Renault, V. M., Jamet, K. and Gilson, E. (2014). Transcriptional outcome of telomere signalling. *Nat. Rev. Genet.* **15**, 491-503. doi:10.1038/nrg3743
- Young, A. J. (2018). The role of telomeres in the mechanisms and evolution of life-history trade-offs and ageing. *Phil. Trans. R. Soc. B* **373**, 20160452. doi:10.1098/rstb.2016.0452
- Zalli, A., Carvalho, L. A., Lin, J., Hamer, M., Erusalimsky, J. D., Blackburn, E. H. and Steptoe, A. (2014). Shorter telomeres with high telomerase activity are associated with raised allostatic load and impoverished psychosocial resources. *Proc. Natl. Acad. Sci. USA* **111**, 4519-4524. doi:10.1073/pnas.1322145111
- Zheng, Q., Huang, J., Wang, G., Cayuela, M. L. and Saretzki, G. C. (2019). Mitochondria, Telomeres and Telomerase Subunits. *Front. Cell Dev. Biol.* **7**, 1-10. doi:10.3389/fcell.2019.00274